

# Aggregating Privacy-Conscious Distributed Energy Resources for Grid Service Provision

Jun-Xing Chin, *Student Member, IEEE*, Andrey Bernstein, *Member, IEEE*,  
and Gabriela Hug, *Senior Member, IEEE*

**Abstract**—With the increasing adoption of advanced metering infrastructure, there are growing concerns with regards to privacy risks stemming from the high resolution measurements. This has given rise to consumer privacy protection techniques that physically alter the consumer’s energy load profile in order to mask private information using localised devices such as batteries or flexible loads. Meanwhile, there has also been increasing interest in aggregating the distributed energy resources (DERs) of residential consumers in order to provide services to the grid. In this paper, we propose a distributed algorithm to aggregate the DERs of privacy-conscious consumers to provide services to the grid, whilst preserving the consumers’ privacy. Results show that the optimisation solution from the distributed method converges to one close to the optimum computed using an ideal centralised solution method, balancing between grid service provision, consumer preferences and privacy protection. While the overall performance of the distributed method lags that of a centralised solution, it preserves the privacy of consumers, and does not require high-bandwidth two-way communications infrastructure.

**Index Terms**—Ancillary Services, Consumer Privacy, Online Gradient Descent, Mutual Information, Optimisation Methods, Smart Meter, Advanced Metering Infrastructure

## I. INTRODUCTION

In recent years, the adoption rate of advanced metering infrastructure (AMI) using smart meters (SMs) has risen steadily across the globe as part of grid modernisation efforts. As of January 2017, 52% of the 150 million electricity consumers in the US have AMI [1], while in Europe, 13 member states are expected to have AMI adoption rates of over 95% by 2020 [2]. In Switzerland, 80% of all electricity meters are to be replaced with SMs by 2027 [3]. AMI provides high-frequency energy consumption measurements to utility operators, allowing for data-driven grid management and planning techniques that promise to improve grid efficiency and transparency. However, this data also entails serious privacy risks for consumers, as it reveals their detailed electricity consumption profiles. It has been shown in the literature that lifestyle patterns, potential illnesses, religious practices, socio-demographic profile, and even appliances used can be inferred from AMI data through data analytics and non-intrusive load monitoring techniques [4]–[8].

These risks and recent developments in consumer privacy protection laws such as the European Union’s General Data

Protection Regulation [9], have spurred the development of privacy-enhancing methods for consumers with AMI, which can be split into two categories: *smart meter data manipulation* (SMDM) and *user demand shaping* (UDS) [10]. SMDM involves pre-processing the AMI data before it is reported, e.g., data aggregation, data anonymisation, and data obfuscation. UDS, on the other hand, entails physically shaping the consumer demand such that the grid-visible load, *i.e.*, the *grid load* no longer reveals private information present in the actual *consumer load*. This is achieved by using behind-the-meter resources such as energy storage devices, flexible loads, and distributed energy sources. While the former may be cheaper to implement, they may impact the utility of the AMI data due to the distortion in the meter readings or may require trusted third parties, e.g. as proposed in [11], [12]. Moreover, as they do not tackle the issue on the physical level, *i.e.*, the actual energy flow, it might be possible to still decipher the actual consumption depending on the protection used [13].

One of the first UDS schemes is described in [14], where the authors implement a best effort scheme to keep the grid load constant. However, this has been shown to leak information whenever there is a change in grid load [15], and has since been followed up by more complex schemes such as [16]–[19]. In [16], the authors propose a differential-privacy based protection scheme using an ideal battery to mask the on/off status of appliances while being cost-friendly. Using a model-distribution predictive control (MDPC) scheme that balances between minimising energy cost and a proxy for privacy loss, the authors in [17] show that a home energy controller can be designed to directly minimise an approximate of mutual information between the grid and consumer loads. And in [18], the authors propose Q-learning based privacy-enhancing control policies using electric vehicles (EVs), flexible thermal loads, and energy storage devices to overcome limitations in modelling consumer load statistics. The control policies are tested on simulated load profiles with an ideal battery and a linearised thermal load model, and show that reasonable privacy-cost trade-off can be achieved by combining a small battery with EVs and an air conditioning device. The authors in [19] derived fundamental bounds on mutual information privacy for consumers with renewable energy sources (RES), both with and without an infinite battery, and proposed a sub-optimal privacy-enhancing scheme for realistic cases (finite battery) based on stochastic gradient descent. Note that in the absence of a battery, privacy can be enhanced through the curtailment of the available RES production.

Meanwhile, the increasing availability of behind-the-meter resources, a.k.a. distributed energy resources (DERs), coupled

This work was supported in part by the *Swiss National Science Foundation* for the COPEs project under the CHIST-ERA Resilient Trustworthy Cyber-Physical Systems (RTCPS) initiative.

J.X. Chin, and G. Hug are with the Power Systems Laboratory, ETH Zurich, 8092 Zurich, Switzerland. Email: {chin | hug}@eeh.ee.ethz.ch. A. Bernstein is with the National Renewable Energy Laboratory, Golden, CO 80401, USA. Email: Andrey.Bernstein@nrel.gov

with the roll-out of smart grid communications infrastructure has spurred the development of demand-side management for smaller loads. Residential consumers, which have traditionally been neglected due to their size, are being aggregated in order to provide services to the grid. Residential demand side aggregation (RDSA) schemes can be divided into two main classes: direct load control, and incentive (signal) based schemes. The authors in [20] provide an overview of incentive based RDSA literature, and propose a multi-agent non-cooperative game framework for integrating RDSA schemes with home energy management systems (HEMSs). Nonetheless, limitations in communications infrastructure remain a challenge for most RDSA schemes [21]. One possible solution is the broadcast of a common signal as suggested in [22], though the design of the signal is still an active field of research; see, e.g. [23] and pertinent references therein.

UDS privacy protection methods, by their nature, lend themselves well to being a part of an RDSA scheme given their inherent flexibility to alter grid load. Moreover, it is intuitive that privacy-aware consumers with UDS protection be considered potential DERs that can be aggregated to provide services to the grid. However, there are only few works on the design of privacy-centric HEMSs for RDSA schemes, with most works focusing solely on the auction activation, or (and) accounting mechanisms, e.g., [24]–[26]. These works employ different cryptographic techniques in the RDSA mechanism in order ensure privacy while being able to attribute rewards to demand response participants, but do not provide designs for the automated HEMSs. In this paper, we design a HEMS for RDSA that also considers the consumers' preferences and real-time privacy loss, without the need for pervasive real-time AMI metering and two-way high-bandwidth communications infrastructure. Using an online projected gradient descent approach proposed in [27], the mechanism preserves the privacy of consumers through UDS and omits the need for real-time measurements from each consumer. Note that the allocation of rewards to individual consumers is not considered in this paper and will be left to future work.

The rest of this paper is organised as follows: Section II details the problem considered, Section III introduces the distributed solution method, Section IV presents and discusses simulation results and Section V concludes the paper, and presents an outlook for future work.

## II. PROBLEM FORMULATION AND SYSTEM DESCRIPTION

We consider the problem of a HEMS that is part of an RDSA scheme and is required to consider the consumer's preferences, and also real-time privacy-loss. Each consumer household consists of a DER, an HEMS controller, and a smart meter that is able to provide high-frequency measurements locally, but unable or unwilling to provide real-time high-frequency remote measurements to the utility provider or aggregator. The aggregator could be a distribution system operator or a third-party energy services provider that has the capability to broadcast high-speed uni-directional signals to each consumer, and is able to measure the real-time aggregated energy consumption of its consumers, e.g., at the sub-station or transformer. The general aggregator system setup is illustrated in Fig. 1(a). We consider the case of the DER being a battery

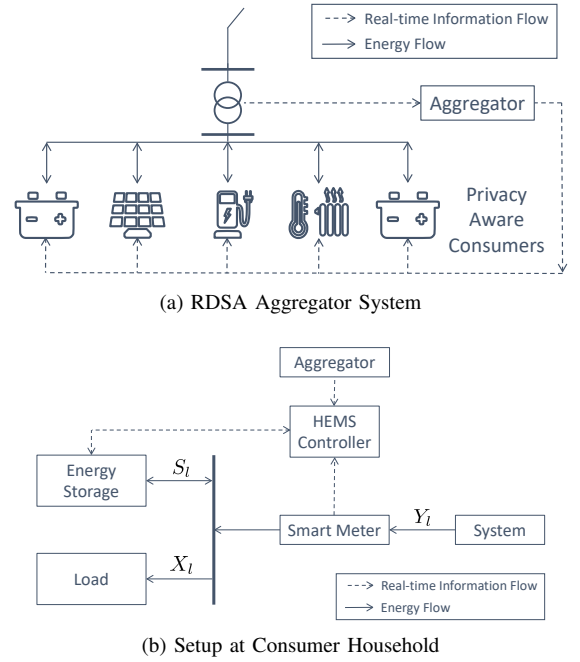


Fig. 1. System setup at consumer households and the aggregator system

in this paper, but the proposed method can easily be extended to incorporate other DERs with convex models. Fig. 1(b) illustrates the system considered at each consumer household. The problem can be framed as solving the following optimisation program:

$$\begin{aligned} & \underset{y_l}{\text{minimise}} && \sum_{l=1}^N \{ \Lambda(y_l) + \mu_l \Phi(y_l) \} + \rho \Gamma(\mathbf{y}) \\ & \text{subject to} && y_l \in \mathcal{F}_l, \quad l = 1, \dots, N, \end{aligned} \quad (1)$$

where  $N$  is the number of consumers in the aggregation,  $y_l$  and  $\mu_l$  are the grid load and price of privacy loss for consumer  $l$ , respectively,  $\Lambda(y_l)$  is the consumer's utility (preference) function,  $\Phi(y_l)$  is a measure of real time privacy-loss,  $\rho$  is the coefficient for grid service provision,  $\Gamma(\mathbf{y})$  gives a measure of the grid service provided (e.g., target load or ancillary service tracking signal), and  $\mathbf{y} := [y_1, y_2, \dots, y_N]^T$  is a vector of consumer grid loads. The set  $\mathcal{F}_l$ , defined by the constraints:

$$0 \leq s_l^+ \leq s_l^{+,max} \quad (2)$$

$$0 \leq s_l^- \leq s_l^{-,max} \quad (3)$$

$$0 \leq e_l + \Delta t (\eta_l s_l^+ - \frac{1}{\eta_l} s_l^-) \leq e_l^{cap} \quad (4)$$

$$y_l = x_l + s_l^+ - s_l^- \quad (5)$$

$$y_l^{min} \leq y_l \leq y_l^{max} \quad (6)$$

enforces the system constraints for consumer  $l$ . Here,  $s_l^+$ ,  $s_l^-$  denote the battery's charging and discharging power;  $s_l^{+,max}$ ,  $s_l^{-,max}$  denote the battery's maximum discharging and charging power rating;  $\eta_l$  denotes the battery's charge/discharge efficiency;  $e_l$  is the battery state of charge;  $e_l^{cap}$  is the battery capacity;  $y_l^{min}$  and  $y_l^{max}$  are the minimum and maximum allowable grid loads;  $x_l$  denotes the instantaneous consumer load; and  $\Delta t$  is the time interval between each control action.

For the rest of the paper,  $A_l$  denotes a random variable,  $a_l$  denotes its realisation, bold letters  $\mathbf{a}$  denote the vector  $[a^1, a^2, \dots]^T$ ,  $\log$  is the base-2 logarithm,  $A^{[t]}$  denotes the sequence  $(A_1, A_2, \dots, A_t)$ ,  $\mathcal{A}$  is the range space for variable  $A$ , and  $p_A(a)$  is the probability of  $A = a$ . The functions  $\Lambda(y_l)$ ,  $\Phi(y_l)$  and  $\Gamma(\mathbf{y})$  are described in the following.

### Consumer Preferences

The function  $\Lambda(y_l)$  can be any convex utility function that reflects the consumer's preferences. For simplicity, we consider a function that penalises deviations from the consumer's day-ahead grid-load schedule, given by

$$\Lambda(y_l) := \|y_l - y_l^{ref}\|_2^2, \quad (7)$$

where  $y_l^{ref}$  is the day-ahead planned consumption. This schedule can include the consumer's preferences on a grid visible load profile, energy cost optimisation and battery state-of-charge requirements.

### Real-Time Privacy Proxy

Mutual information (MI) is widely used as a measure of privacy loss for consumers with AMI [10], [15]. Let  $X_l \in \mathcal{X}_l$  and  $Y_l \in \mathcal{Y}_l$  denote the random variables modelling the instantaneous consumer load and the total grid load, respectively. For the purpose of estimating the MI, we assume that these random variables are discrete and have finite support. In particular,  $\mathcal{X}_l = \{x_l^0, x_l^1, \dots, x_l^m\}$ ,  $\mathcal{Y}_l = \{y_l^0, y_l^1, \dots, y_l^n\}$ , where  $m$  and  $n$  are the number of bins used to quantise the consumer and grid loads, respectively. The MI function for discrete random variables is given by

$$I(X_l; Y_l) := \sum_{x_l \in \mathcal{X}_l} \sum_{y_l \in \mathcal{Y}_l} p_{X_l, Y_l}(x_l, y_l) \log \frac{p_{X_l, Y_l}(x_l, y_l)}{p_{X_l}(x_l)p_{Y_l}(y_l)},$$

where  $p_{X_l, Y_l}$ ,  $p_{X_l}$ , and  $p_{Y_l}$  are the joint and marginal probability distribution functions (PDFs) of the random variables. In order to formulate MI as a function of the next grid load realisations, binary variables  $\mathbf{z}_l = \{z_l^{ij}\}_{i=1, j=1}^{m, n} \in \mathcal{Z}_l = \{0, 1\}^{m \times n}$  are introduced in [17] to relate the grid load variable,  $y_l$  to its statistics. Given that the value of  $x_l$  falls in the  $i$ -th bin, for each value of  $y_l$ , there exists exactly one non-zero  $z_l^{ij}$  representing the bin where  $y_l$  falls. Using  $\mathbf{z}_l$  as the optimisation variables, an approximation of the MI function,  $\tilde{I}(\mathbf{z}_l)$  is then formulated as an optimisation objective [17]. A brief summary on the derivation of  $\tilde{I}(\mathbf{z}_l)$  is provided in online Appendix A [28]; further details can be found in [17]. Here, we relax the binary constraints on  $\mathbf{z}_l$ , *i.e.*  $\mathbf{z}_l \in \mathcal{Z}'_l = [0, 1]^{m \times n}$  and allow that for each value of  $y_l$ , there exists a set of non-zero  $z_l^{ij}$  within the feasible set. Define then the set  $\mathcal{F}'_l$  as the set of all  $(y_l, \mathbf{z}_l)$  that satisfies the constraints (2) to (6), in addition to the following constraints:

$$\sum_{j=1}^n z_l^{i^*j} = 1 \quad (8)$$

$$z_l^{ij} = 0, \quad \forall i \neq i^* \quad (9)$$

$$\sum_{j=1}^n z_l^{i^*j} y_l^{j-1} \leq y_l < \sum_{j=1}^n z_l^{i^*j} y_l^j, \quad (10)$$

where  $i^*$  is the index corresponding to the given value of  $x_l$ . Constraint (10) links the grid load to its PDF estimate. Furthermore, let  $\Phi(y_l) = \tilde{I}(\mathbf{z}_l)$  for any  $\mathbf{z}_l$  satisfying  $(y_l, \mathbf{z}_l) \in \mathcal{F}'_l$ .  $\Phi(y_l)$  is a quadratic form that is strongly convex for  $m > 1$ . This can be implied from [17] by relaxing the binary constraints and limiting the optimisation program to a single time step and can be shown by analysing its algebraically manipulated form (see online Appendix B [28]). Note that  $\Phi(y_l)$  is only strongly convex for  $m > 1$ . Furthermore, the gradient of  $\Phi(y_l)$  is bounded, thereby making  $\Phi(y_l)$  Lipschitz continuous. These properties will be used later to apply the online gradient descent method to solve (1).

### Ancillary Service Provision

We consider the tracking of a target aggregate real power load profile as the ancillary service objective, and penalise deviations from this target profile, *i.e.*,

$$\Gamma(\mathbf{y}) := \left\| \left( \sum_{l=1}^N y_l \right) - \bar{y} \right\|_2^2, \quad (11)$$

where  $\bar{y}$  is the target profile. This target profile can be shaped to provide services such as peak shaving, grid balancing, and congestion alleviation, or simply just to follow a planned consumption profile. Note that one could also track an additional target reactive power profile in order to provide voltage support, but this is left as the subject of future work.

## III. PROJECTED ONLINE GRADIENT DESCENT

The overall optimisation problem is now given by

$$\begin{aligned} & \underset{y_l, \mathbf{z}_l}{\text{minimise}} && \sum_{l=1}^N \{\Lambda(y_l) + \mu_l \Phi(y_l)\} + \rho \Gamma(\mathbf{y}) \\ & \text{subject to} && (y_l, \mathbf{z}_l) \in \mathcal{F}'_l, \quad l = 1, \dots, N, \end{aligned} \quad (12)$$

can be solved optimally using a centralised controller by the aggregator if real-time high-resolution SM data and two-way high-bandwidth communications are available. However, given that current AMI deployments are constrained by communication infrastructure bandwidths, this solution method remains impractical. Moreover, this would also require that private information from all consumers, *i.e.* their actual consumer load, privacy preferences and day-ahead schedules, be revealed to the aggregator, invalidating the privacy protection objective. Therefore, we propose solving (12) using the distributed feedback-based online gradient descent solution method proposed in [27]. The algorithm replaces the coupling of the grid load variables across consumers in (11) with the latest real-time aggregated consumption measurement  $\hat{y}$  at the point of common coupling:

$$\sum_{l=1}^N y_l \approx \hat{y}.$$

Hence, only the value  $\|\hat{y} - \bar{y}\|_2^2$  is communicated in real-time, and is treated as a constant when computing the gradients. This makes (12) separable and solvable locally, overcoming the lack of real-time SM data and mitigating privacy concerns. The availability of  $\hat{y}$  can readily be assumed given the

increasing adoption of phasor measurement units (PMUs), and that transformers or busbars can easily be outfitted with a high-frequency measurement device. The use of  $\hat{y}$  leads to a lagged and sub-optimal solution at each time step. However, by assuming that high-speed control actions can be actuated faster than the time-varying nature of (12), the distributed algorithm is shown to converge to a centralised solution in [27], provided that the optimisation problem is strongly convex.

Recall that (12) is strongly convex for  $m > 1$ . Nevertheless, we add a regularisation term  $\|\mathbf{h}\|_2^2$  with a small coefficient  $\sigma_2/2$ , where  $\mathbf{h}$  is the vector of all the optimisation variables; this ensures that (12) is at least  $\sigma_2$ -strongly convex in all cases (e.g., when  $m = 1$ , or when extending the algorithm to multiple time steps). It is easy to see that  $\|\mathbf{h}\|_2^2$ , which is the sum of the squares of the variables, is separable. Accordingly, let<sup>1</sup>  $\rho = \sigma_1/2$ , and

$$f(y_l, \mathbf{z}_l) = \sum_{l=1}^N \left\{ \Lambda(y_l) + \mu_l \tilde{I}(\mathbf{z}_l) \right\} + \frac{\sigma_1}{2} \Gamma(\mathbf{y}) + \frac{\sigma_2}{2} \|\mathbf{h}\|_2^2.$$

We now solve the following quadratic program,

$$\begin{aligned} & \underset{y_l, \mathbf{z}_l}{\text{minimise}} && f(y_l, \mathbf{z}_l) \\ & \text{subject to} && (y_l, \mathbf{z}_l) \in \mathcal{F}'_l, \end{aligned} \quad (13)$$

locally at each HEMS by first taking a gradient descent step:

$$\tilde{s}_{l,t}^+ = s_{l,t-1}^+ - r \nabla_{s_{l,t}^+} f(y_l, \mathbf{z}_l) \quad (14)$$

$$\tilde{s}_{l,t}^- = s_{l,t-1}^- - r \nabla_{s_{l,t}^-} f(y_l, \mathbf{z}_l) \quad (15)$$

$$\tilde{z}_{l,t}^{i^*j} = z_{l,t-1}^{i^*j} - r \nabla_{z_{l,t}^{i^*j}} f(y_l, \mathbf{z}_l), \quad j = 1, \dots, n, \quad (16)$$

where  $r$  is the gradient descent step size, and  $\nabla_A$  is the gradient with respect to  $A$ . The final solution is then obtained by projecting the interim solution onto the feasible set, *i.e.*,

$$[s_{l,t}^+, s_{l,t}^-, z_{l,t}^{i^*j}]^\top = \text{proj}_{\mathcal{F}'_l} [\tilde{s}_{l,t}^+, \tilde{s}_{l,t}^-, \tilde{z}_{l,t}^{i^*j}]^\top. \quad (17)$$

Only variables  $z_{l,t}^{i^*j}$  are updated at each time step, with variables  $z_{l,t}^{ij}$  for  $i \neq i^*$  being treated as zero when computing the gradients for  $z_{l,t}^{i^*j}$ . Note that the actual values of  $z_{l,t}^{ij}$ ,  $i \neq i^*$  are not re-initialised as zero, and are kept for future time steps in order to ensure convergence. The gradients  $\nabla_{s_{l,t}^+} f(y_l, \mathbf{z}_l)$ ,  $\nabla_{s_{l,t}^-} f(y_l, \mathbf{z}_l)$ , and  $\nabla_{z_{l,t}^{i^*j}} f(y_l, \mathbf{z}_l)$  are derived from (5) and (13), then computed by substituting for  $\hat{y}$ ; see online Appendix B for the details on the gradients [28].

### Battery Modelling

The convex modelling of realistic batteries while avoiding physically infeasible but optimal decisions due to simultaneous charging and discharging remains a research challenge. There are numerous modelling methods, e.g., using binary variables, quadratic constraints, or penalising battery use, but they are either non-convex, or are inapplicable because simultaneous charging and discharging is allowed and is optimal for  $\Phi(y_l)$  in some scenarios. To circumvent this issue, we assume that the

battery is unable to go directly from charging to discharging, *i.e.*, it must go through “zero”,

$$(s^+ > 0, s^- = 0) \rightarrow (s^+ = 0, s^- = 0) \rightarrow (s^+ = 0, s^- > 0),$$

and vice versa. This is a reasonable assumption given sufficiently fast control actions and limitations on certain power converter designs.

The proposed distributed projected online gradient descent algorithm incorporating this battery modelling work-around is summarised in Algorithm 1. We note that the convergence of this algorithm is guaranteed provided that the step size  $r$  in (14) - (16) is small enough; see [27] for details.

---

#### Algorithm 1 algorithm for solving (13) at time $t$

---

- 1: obtain aggregated load measurement  $\hat{y}_{t-1}$
  - 2: obtain target load  $\bar{y}_t$
  - 3: compute  $\|\hat{y}_{t-1} - \bar{y}_t\|_2^2$  and broadcast to consumers
  - 4: **for** consumer 1 to  $N$  **do**
  - 5:   obtain load forecast  $x_{l,t}$  and battery state  $e_{l,t}$
  - 6:   **if** charge flag = true **then**
  - 7:     compute  $s_{l,t}^+$  and  $z_{l,t}^{i^*j}$  using (14), (16) and (17)
  - 8:     **if**  $s_{l,t}^+ \geq 0$  **then**
  - 9:       actuate  $s_{l,t}^+$  and update  $z_{l,t}^{i^*j}$
  - 10:     **else**
  - 11:       charge flag = false
  - 12:       actuate  $s_{l,t}^+ = 0$  and update  $z_{l,t}^{i^*j}$
  - 13:     **else**
  - 14:       compute  $s_{l,t}^-$  and  $z_{l,t}^{i^*j}$  using (15), (16) and (17)
  - 15:       **if**  $s_{l,t}^- \geq 0$  **then**
  - 16:         actuate  $s_{l,t}^-$  and update  $z_{l,t}^{i^*j}$
  - 17:       **else**
  - 18:         charge flag = true
  - 19:         actuate  $s_{l,t}^- = 0$  and update  $z_{l,t}^{i^*j}$
  - 20:       update constants ( $a_l^{ij}$ ,  $b_l^j$ ,  $c_l^i$ ) used in the MI
  - 21:       approximation (see Appendix A in [28] for details)
  - 22: **advance** to  $t + 1$
- 

## IV. NUMERICAL EXPERIMENTS

The proposed scheme is tested using 1 Hz smart meter data taken from the ECO dataset [29]. As there are only five houses in this dataset, we emulated more consumers in the RDSA scheme by drawing data from multiple days over the period between 26 August and 9 September, 2012 from the five households.

### Simulation Setup

Each household in the RDSA scheme was assigned a random price of privacy loss,  $1 \leq \mu_l \leq 9$ , to mimic the behaviour of multiple real households. To enforce the assumption that control actions are actuated faster than the time varying nature of (13), we assume that the local high frequency SM measurements have a resolution of 0.2 Hz, and that the target grid signal also varies every 5 seconds, while the aggregated load measurements are available every second. Each household tracks an arbitrary day-ahead schedule,  $y_l^{ref}$ ,

<sup>1</sup>for simplicity in deriving the gradient

TABLE I  
INDIVIDUAL HOUSEHOLD SYSTEM PARAMETERS

Real-Time PDF Estimation Sample Size, $K$	901
Number of $\mathcal{X}$ Bins, $m$	15
Number of $\mathcal{Y}$ Bins, $n$	15
Additive Smoothing, $\varepsilon$	0.1
Battery Capacity	6.4 kWh
Battery Power	3.3 kW
Battery Efficiency, $\eta$	96 %
RDSA Reserve Capacity, $\gamma$	0.15 kW

TABLE II  
GENERAL SIMULATION PARAMETERS

Initial Battery State of Charge	3.2 kWh
Ancillary Service Coefficient, $\sigma_1$	5
Regularisation Coefficient, $\sigma_2$	$1e^{-4}$
Descent Step Size, $r$	0.012
No. of Consumers, $N$	20

computed using a single multi-time step optimisation for energy costs and MI privacy, at half-hourly resolution with the MDPC algorithm described in [17], and on a two-tier time-of-use energy tariff. Here, we define  $\hat{y} = \sum_{l=1}^N y_l$  for simplicity, omitting grid losses, and assume that grid in-feed is not allowed, *i.e.*,  $y_l^{min} = 0$ . Depending on network topology and size, the grid losses may impact the RDSA scheme's performance in reality, but this is outside the scope of this paper. The general system setup at each consumer household is summarised in Table I. The target aggregate load  $\bar{y}$  is generated using the aggregated day-ahead consumer schedules as a base, considering total RDSA reserve capacity  $\bar{\gamma} = N\gamma$ . For ease of assessment, this is designed such that the target load is energy neutral with respect to the aggregate day-ahead schedule within each half-hourly interval. When generating such a reference curve, we took into account battery losses (max bias of 0.1% of reserve capacity), and ensured that the aggregate reserves are sufficient to meet the ancillary service requests approximately 99.7% of the time.

Unless otherwise stated, the simulation parameters are as listed in Table II where applicable. For ease of comparison and simplicity, we set aside battery energy capacity corresponding to  $\gamma$  at each consumer household in their day-ahead schedules, and assume that the battery model in the optimisation problem is accurate. The proposed distributed algorithm (abbreviated as Dist.POGD in this section) is compared against an ideal centralised solution for (13), both with and without relaxing the binary constraints on  $z_l$ , by modelling it in YALMIP [30], and solving it with the Gurobi solver. For the distributed algorithm, we assume a persistent forecast for  $x_l$ , *i.e.*, use the latest high-frequency SM measurement for computing the gradient step, while using a perfect forecast for the centralised

TABLE III  
VARIABLES USED IN THE OPTIMISATION PROBLEM AT TIME  $t$

	Distributed	Centralised
Load Forecast	$x_{l,t-1}$	$x_{l,t}$
Target Aggregate Load	$\bar{y}_{l,t}$	$\bar{y}_{l,t}$
Day-Ahead Schedule	$y_{l,t}^{ref}$	$y_{l,t}^{ref}$
Aggregate Load	$\hat{y}_{l,t-1}$	$\sum_{l=1}^N y_{l,t}$

solution. Note that  $\sum_{l=1}^N y_l$  is not substituted with  $\hat{y}$  in the centralised solution. Table III summarises the information used in the respective solution methods at time  $t$ .

### Results and Discussion

Fig. 2 illustrates the target aggregate load profile, the aggregated grid loads from Dist.POGD and a centralised solution with relaxed binary constraints, and the total consumer load. Within the specific illustrated period, the batteries are discharging, resulting in grid loads less than the total consumer load; but the converse can be true in other periods. Using the parameters in Table II and the selected energy and privacy loss prices, the Dist.POGD solution converges close to the ideal centralised solution, as seen in Fig. 2, and overshoots only when there is a significant consumer load change. The performance of Dist.POGD is affected by the choice of parameters in Table II. These parameters have to be chosen empirically in a real system, as consumer privacy preferences would be unknown to the aggregator.

Numerically, we evaluate the performance of the algorithms over a period of three and a half hours (number of samples  $K_s = 12600$ ; simulate four hours, discard the first half-hour for initialisation purposes) with the following metrics. For ancillary service provision, the algorithms are evaluated based on the normalised root mean square error (NRMSE) between  $\hat{y}$  and  $\bar{y}$ , given by

$$\text{NRMSE} := \frac{\sqrt{\frac{1}{K_s} \sum_{k=1}^{K_s} (\hat{y}_k - \bar{y}_k)^2}}{\bar{y}^{mean}} \times 100\% ,$$

$$\bar{y}^{mean} = \frac{1}{K_s} \sum_{k=1}^{K_s} \bar{y}_k ,$$

and the mean absolute percentage error (MAPE),

$$\text{MAPE} := \frac{100\%}{K_s} \sum_{k=1}^{K_s} \left| \frac{\hat{y}_k - \bar{y}_k}{\bar{y}_k} \right| .$$

MAPE gives the average of the errors at each time  $t$ , while NRMSE emphasises large deviations from the target load, which are undesirable, and reflects the target load tracking error relative to the overall mean. The consumer preference (day-ahead schedule tracking) is evaluated by computing its normalised mean absolute error (NMAE), *i.e.*, the absolute error as a percentage of the maximum grid load,

$$\text{NMAE} := \frac{100\%}{K_s y_l^{max}} \sum_{k=1}^{K_s} \left| y_{l,k} - y_{l,k}^{ref} \right| .$$

We used an approximate MI function in the objective function of the optimisation problem. However, for evaluation purposes we estimate the average MI, assuming identical and independently distributed random variables (denoted as *IID*), and stationary Markov processes (denoted as *Markov*), as described in [31], [32]. Such evaluation requires the computation of  $p_{X,Y}(x,y) \log[p_{X,Y}(x,y)/p_X(x)p_Y(y)]$ , which in the case of  $p_{X,Y}(x,y)$  being zero, is set to zero to avoid computing log 0. The Markov MI captures some of the time correlation between the consumer and grid loads, which is neglected when

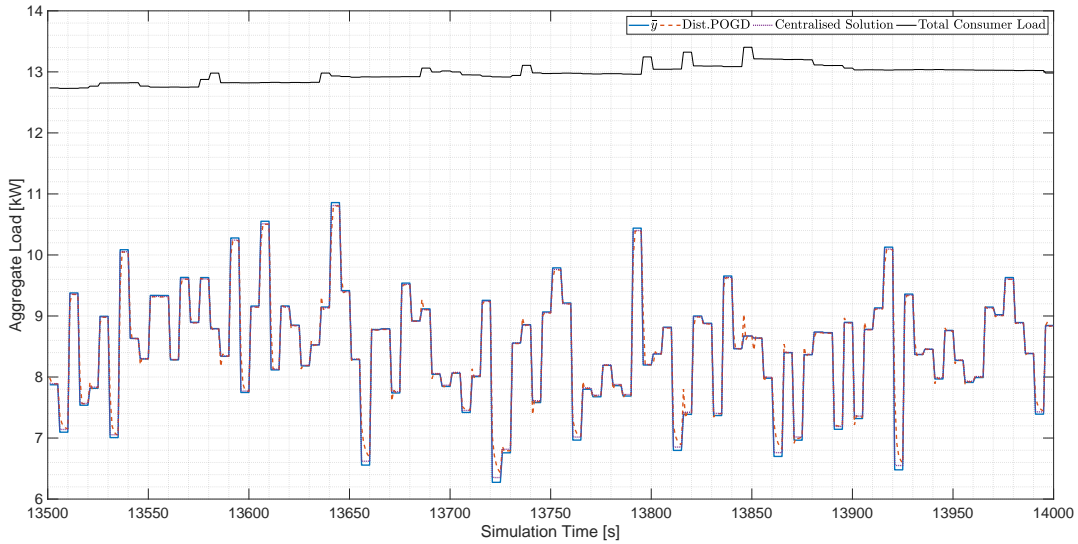


Fig. 2. Target grid load, and aggregated grid and consumer loads

calculating the IID MI [32]. Note that while modelling the  $X_l$  and  $Y_l$  as time-varying Markov processes would yield more accurate MI estimates, there are insufficient samples from this simulation for its application.

Privacy risks are time resolution dependent, *i.e.*, the resolution at which consumers are metered influences their privacy risks [33]. Therefore, the MI is also assessed at 1-minute resolution, given that this metering resolution is more likely to be deployed than 1-second measurements.

In our case study, we assume that the aggregator has the following information: the ancillary service provision signal  $\|\hat{y}_{t-1} - \bar{y}_t\|_2^2$ , and each consumer's day-ahead schedule  $y_l^{ref}$ . Each consumer's grid load on the other hand is composed of their day-ahead schedule, deviations due to privacy-protection, ancillary service request, and consumer load deviations from day-ahead forecasts. Hence, the MI needs to be evaluated for grid load profiles with the ancillary service portion removed (denoted as *GS* or  $y_l'$ ) and the day-ahead schedule subtracted (denoted as *DAGS* or  $y_l''$ ):

$$y_l' = y_l - \underbrace{(\hat{y} - \bar{y}) \frac{y_l^{mean}}{\sum_{l=1}^N y_l^{mean}}}_{\text{ancillary service request}},$$

$$y_l^{mean} = \frac{1}{K_s} \sum_{k=1}^{K_s} y_{l,k},$$

$$y_l'' = y_l' - y_l^{ref}.$$

Fig. 3 illustrates the original and adjusted grid loads for consumer 1. Note that the ancillary service request does not equal the ancillary service provision, and that  $y_l''$  is the aggregator's guess that does not reflect the actual consumer load. The number of bins,  $m$  and  $n$ , are kept the same as in the optimisation problem when computing the MI between  $x_l$  and  $y_l$ , but  $n$  is doubled when computing the MI for  $y_l'$  and  $y_l''$  to account for the possible negative values. All else being equal, increasing the number of bins generally leads to an increase in the MI estimate as discussed in [17].

Tables IV and V summarise the performance of Dist.POGD with different parameters, and the two centralised solutions.

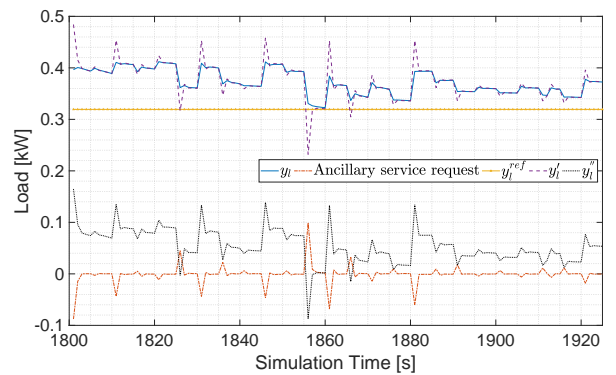


Fig. 3. Grid load for consumer 1

While the Dist.POGD solution converges close to the ideal centralised solution as seen in Fig. 2, there is a deterioration in the overall performance due to the time required for convergence, forecast error, and the replacement of  $\hat{y}_{l,t-1}$  for  $\sum_{l=1}^N y_{l,t}$ . The use of a persistence forecast in Dist.POGD instead of a perfect forecast allows for a better analysis of its performance if deployed in reality. Relaxing the binary constraints on  $\mathbf{z}_l$  marginally improves the NRMSE, MAPE, average NMAE, and most of the MI estimates, showing that this relaxation does not significantly impact the performance of the MI approximate in the objective function for a single control action. Note, however, that this may not be true in general; in fact, the opposite might occur. One can also see a deterioration in privacy protection if privacy risks are assessed at a resolution lower than the controller's, *e.g.* at one minute instead of one second. Note also that the 1-sec Markov MI values are very small because the measure is unable to fully capture the time-correlated privacy leakage that it was designed for. The time-correlation of the load profiles is at least 5 seconds. This drawback is highlighted in [32]. Moreover, correcting for the ancillary service request results in higher 1-sec Markov MI, and 1-min IID and Markov MI estimates, thus resulting in more leakage of private information. However, further compensating for the day-ahead schedule does not reveal additional private information (compared to  $y_l'$ ). This shows that the ancillary service request signal constitutes

TABLE IV  
PERFORMANCE OF DIFFERENT SOLUTION METHODS AND PARAMETERS

	NRMSE	MAPE	Avg. NMAE
Reference Dist.POGD	1.694%	0.7878%	4.699%
Centralised, binary	0.336%	0.295%	3.71%
Centralised, relaxed	0.322%	0.283%	3.53%
15 Consumers	2.69%	1.61%	5.42%
25 Consumers	1.51%	0.827%	4.32%
$r = 0.008$	2.80%	1.63%	5.13%
$r = 0.016$	1.56%	0.914%	4.41%
$\sigma_2 = 0$	1.691%	0.7873%	4.695%
$\sigma_2 = 0.001$	1.694%	0.7883%	4.703%
$\mu_l = 0$	1.68%	0.777%	4.61%
$11 \leq \mu_l \leq 19$	1.78%	0.866%	5.21%
$K = 600$	1.70%	0.796%	4.71%
$K = 1200$	1.69%	0.785%	4.69%
$\sigma_1 = 3$	3.17%	2.05%	4.41%
$\sigma_1 = 7$	1.65%	0.978%	4.86%

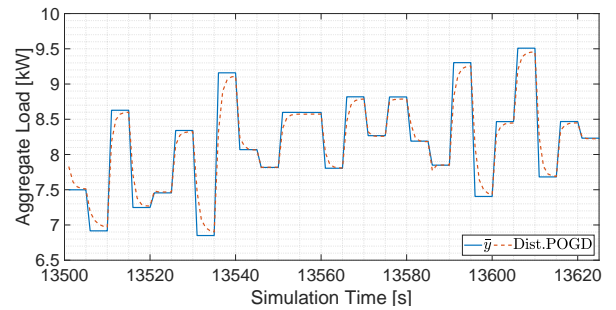
sensitive side-information, while additional information on the day-ahead schedule may not exacerbate consumer privacy loss. Further study on ways of incorporating the day-ahead schedule is needed for a conclusive verdict on its privacy sensitivity.

As discussed, the RDSA parameters are setup-dependent, and changing the number of consumers in the RDSA while keeping all else constant affects the convergence rates and performance. This is illustrated for 25 and 15 consumers in Fig. 4. The choice of gradient descent step size  $r$  affects the convergence rate of Dist.POGD; too high a value for  $r$  leads to overshoots and instability, while too low a value hinders convergence to the optimal solution before the problem changes, as seen in Fig. 5. 1-Sec Markov MI increases with larger step sizes (see Table V), showing an increase in the leakage of time-correlated private information with larger  $r$  values. On the other hand, the overall tracking performance improves and IID MI decreases as the rate of convergence (and overshoots) increases (see Table IV and Fig. 5). An ideal value for the coefficient  $\sigma_2$  for the regularisation term  $\|\mathbf{h}\|_2^2$  would result in minimal impact on the performance of the algorithm. As seen in Tables IV and V, Dist.POGD with  $\sigma_2 = 1e^{-4}$  has similar performance to an algorithm without regularisation.

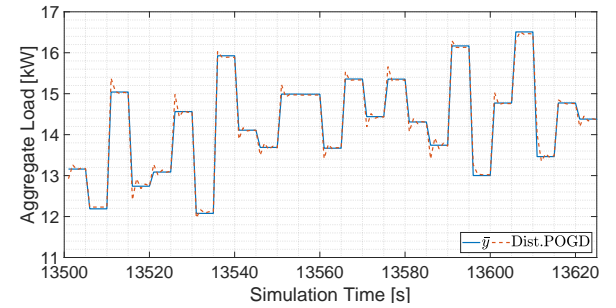
As expected, increasing  $\sigma_1$  reduces the ancillary service provision NRMSE at the expense of increasing the day-ahead tracking NMAE and most MI estimates. However, a decrease in  $\sigma_1$  does not necessarily lead to a decrease in IID MI due to a slower convergence rate (see Fig. 6). Surprisingly, increasing  $\sigma_1$  could also lead to an increase in ancillary service provision MAPE due to tracking overshoots as illustrated in Fig. 6. Increasing  $\mu_l$  decreases IID MI, but increases ancillary service provision NRMSE and MAPE, and the average NMAE for tracking the day-ahead NMAE. Changing the sample size  $K$  in the objective function has a similar effect to changing  $\mu_l$  as it increases the importance of the current control action in estimating the PDF of  $(X_i, Y_i)$ . However, their effects are not equivalent as reducing  $K$  could lead to overfitting the PDF.

## V. CONCLUSION

In this paper, a distributed projected online gradient descent algorithm for providing ancillary services to the grid by aggregating privacy-conscious residential consumers was presented. A balance between the different objectives can be achieved by adjusting their weights. Despite minor performance degradation when compared to an ideal centralised



(a) 15 consumers



(b) 25 consumers

Fig. 4. Tracking performance with different aggregation sizes

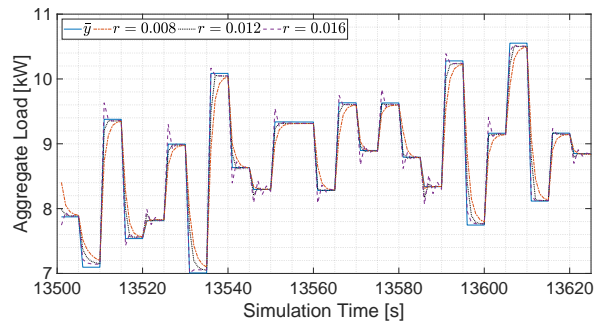


Fig. 5. Comparison between different step sizes,  $r$

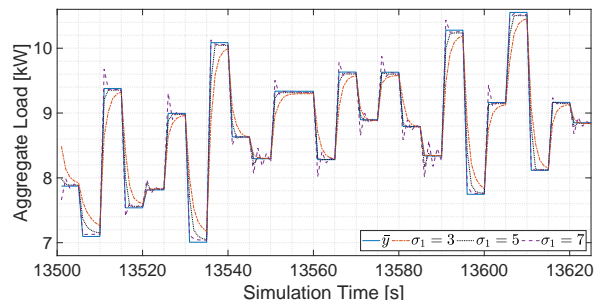


Fig. 6. Comparison between different tracking coefficients,  $\sigma_1$

aggregation scheme, the proposed algorithm does not require high-bandwidth communications infrastructure. Moreover, it allows for the preservation of consumer privacy as the actual consumer load does not need to be revealed to the aggregator.

Future work will focus on the provision of other grid services such as voltage support, incorporating DERs with uncertainty or more complex constraints, and considering grid constraints in the optimisation problem.

## REFERENCES

- [1] U.S. Energy Information Administration, "Annual electric power

TABLE V  
MUTUAL INFORMATION FROM DIFFERENT SOLUTION METHODS AND PARAMETERS

	Avg. 1 Sec		Avg. 1 Min		Avg. 1 Sec GS		Avg. 1 Min GS		Avg. 1 Sec DAGS		Avg. 1 Min DAGS	
	IID	Markov	IID	Markov	IID	Markov	IID	Markov	IID	Markov	IID	Markov
Reference Dist.POGD	0.248	0.020	0.280	0.193	0.246	0.049	0.407	0.399	0.089	0.038	0.212	0.360
Centralised, binary	0.236	0.018	0.277	0.140	0.233	0.050	0.371	0.334	0.062	0.039	0.179	0.406
Centralised, relaxed	0.221	0.015	0.270	0.147	0.225	0.049	0.358	0.342	0.046	0.033	0.166	0.417
15 Consumers	0.301	0.018	0.354	0.228	0.295	0.044	0.478	0.413	0.101	0.033	0.236	0.371
25 Consumers	0.223	0.020	0.244	0.164	0.224	0.051	0.360	0.328	0.088	0.037	0.188	0.307
$r = 0.008$	0.256	0.019	0.300	0.194	0.251	0.046	0.414	0.392	0.098	0.037	0.214	0.356
$r = 0.016$	0.247	0.022	0.279	0.184	0.243	0.055	0.407	0.388	0.085	0.040	0.211	0.361
$\sigma_2 = 0$	0.248	0.020	0.281	0.192	0.246	0.049	0.409	0.401	0.089	0.038	0.208	0.360
$\sigma_2 = 0.001$	0.247	0.020	0.281	0.192	0.246	0.049	0.408	0.400	0.089	0.038	0.212	0.361
$\mu_l = 0$	0.254	0.020	0.287	0.194	0.251	0.049	0.413	0.399	0.088	0.037	0.202	0.360
$11 \leq \mu_l \leq 19$	0.237	0.020	0.269	0.196	0.234	0.049	0.399	0.422	0.087	0.038	0.227	0.388
$K = 600$	0.247	0.020	0.276	0.196	0.246	0.048	0.403	0.407	0.088	0.037	0.210	0.360
$K = 1200$	0.248	0.020	0.282	0.196	0.247	0.049	0.408	0.396	0.090	0.038	0.211	0.353
$\sigma_1 = 3$	0.253	0.018	0.294	0.189	0.248	0.045	0.403	0.398	0.089	0.034	0.210	0.354
$\sigma_1 = 7$	0.250	0.023	0.285	0.204	0.244	0.057	0.416	0.411	0.090	0.043	0.215	0.367

- industry report, form EIA-861." 2017. [Online]. Available: [https://www.eia.gov/electricity/annual/html/epa\\_10\\_10.html](https://www.eia.gov/electricity/annual/html/epa_10_10.html)
- [2] European Commission, "Cost-benefit analyses & state of play of smart metering deployment in the EU-27," 2014. [Online]. Available: <https://eur-lex.europa.eu/legal-content/EN/TXT/PDF/?uri=CELEX:52014SC0189&from=EN>
- [3] Swiss Federal Office of Energy, "Wichtigste Neuerungen im Energierecht ab 2018," 2017. [Online]. Available: <https://www.news.admin.ch/news/message/attachments/50166.pdf>
- [4] T. Hargreaves, M. Nye, and J. Burgess, "Making energy visible: A qualitative field study of how householders interact with feedback from smart energy monitors," *Energy Policy*, vol. 38, no. 10, 2010.
- [5] A. Molina-Markham, P. Shenoy, K. Fu, E. Cecchet, and D. Irwin, "Private memoirs of a smart meter," in *Proceedings of the 2nd ACM Workshop on Embedded Sensing Systems for Energy-Efficiency in Building*, Zurich, Switzerland, Nov. 2010, pp. 61–66.
- [6] P. McDaniel and S. McLaughlin, "Security and privacy challenges in the smart grid," *IEEE Security and Privacy*, vol. 7, no. 3, 2009.
- [7] Y. Wang, Q. Chen, D. Gan, J. Yang, D. S. Kirschen, and C. Kang, "Deep learning-based socio-demographic information identification from smart meter data," *IEEE Trans. on Smart Grid*, 2018, to be published.
- [8] V. Becker and W. Kleiminger, "Exploring zero-training algorithms for occupancy detection based on smart meter measurements," *Computer Science - Research and Development*, vol. 33, no. 1-2, 2018.
- [9] European Union, "Regulation (EU) 2016/679 of the European Parliament and of the Council of 27 April 2016 on the protection of natural persons with regard to the processing of personal data and on the free movement of such data, and repealing Directive 95/46/EC (General Data Protection Regulation)," *Official J. of the European Union*, May 2016.
- [10] G. Giacconi, D. Gündüz, and H. V. Poor, "Privacy-aware smart metering: Progress and challenges," *IEEE Signal Processing Magazine*, vol. 35, no. 6, pp. 59–78, Nov. 2018.
- [11] C. Efthymiou and G. Kalogridis, "Smart grid privacy via anonymization of smart metering data," in *2010 First IEEE International Conference on Smart Grid Communications*, Gaithersburg, MD, USA, Oct. 2010.
- [12] C. Rottondi, G. Mauri, and G. Verticale, "A data pseudonymization protocol for smart grids," in *2012 IEEE Online Conference on Green Communications (GreenCom)*, Sept. 2012.
- [13] M. Jawurek, M. Johns, and K. Rieck, "Smart metering de-pseudonymization," in *27th Annual Computer Security Applications Conference on - ACSAC '11*, Orlando, FL, USA, Dec. 2011.
- [14] G. Kalogridis, C. Efthymiou, S. Z. Denic, T. A. Lewis, and R. Cepeda, "Privacy for Smart Meters: Towards Undetectable Appliance Load Signatures," in *First IEEE International Conference on Smart Grid Communications (SmartGridComm)*, 2010, pp. 232–237.
- [15] W. Yang, N. Li, Y. Qi, W. Qardaji, S. McLaughlin, and P. McDaniel, "Minimizing private data disclosures in the smart grid," in *Proceedings of the 19th ACM conference on computer and communications security (CCS '12)*, Raleigh, North Carolina, USA, Oct. 2012.
- [16] Z. Zhang, Z. Qin, L. Zhu, J. Weng, and K. Ren, "Cost-friendly differential privacy for smart meters: Exploiting the dual roles of the noise," *IEEE Trans. on Smart Grid*, vol. 8, no. 2, pp. 619–626, 2017.
- [17] J. X. Chin, T. Tinoco De Rubira, and G. Hug, "Privacy-protecting energy management unit through model-distribution predictive control," *IEEE Trans. on Smart Grid*, vol. 8, no. 6, pp. 3084–3093, 2017.
- [18] Y. Sun, L. Lampe, and V. W. S. Wong, "Smart meter privacy: Exploiting the potential of household energy storage units," *IEEE Internet of Things Journal*, vol. 5, no. 1, pp. 69–78, 2018.
- [19] G. Giacconi, D. Gündüz, and H. V. Poor, "Smart meter privacy with renewable energy and an energy storage device," *IEEE Trans. on Information Forensics and Security*, vol. 13, no. 1, pp. 129–142, 2018.
- [20] A. C. Chapman, G. Verbic, and D. J. Hill, "Algorithmic and strategic aspects to integrating demand-side aggregation and energy management methods," *IEEE Trans. on Smart Grid*, vol. 7, no. 6, 2016.
- [21] A. Rajabi, L. Li, J. Zhang, and J. Zhu, "Aggregation of small loads for demand response programs implementation and challenges: A review," in *2017 IEEE Intl. Conference on Environment and Electrical Engineering and 2017 IEEE Industrial and Commercial Power Systems Europe (EEEIC / I&CPS Europe 2017)*, Milan, Italy, June 2017.
- [22] D. S. Callaway and I. A. Hiskens, "Achieving controllability of electric loads," *Proceedings of the IEEE*, vol. 99, no. 1, pp. 184–199, 2011.
- [23] A. Bernstein and E. Dall'Anese, "Real-time feedback-based optimization of distribution grids: A unified approach," *IEEE Transactions on Control of Network Systems*, 2017, to be published. [Online]. Available: <https://arxiv.org/abs/1711.01627>
- [24] H. Li, X. Lin, H. Yang, X. Liang, R. Lu, and X. Shen, "EPPDR: An efficient privacy-preserving demand response scheme with adaptive key evolution in smart grid," *IEEE Trans. on Parallel and Distributed Systems*, vol. 25, no. 8, pp. 2053–2064, 2014.
- [25] Y. Gong, Y. Cai, Y. Guo, and Y. Fang, "A privacy-preserving scheme for incentive-based demand response in the smart grid," *IEEE Trans. on Smart Grid*, vol. 7, no. 3, pp. 1304–1313, 2016.
- [26] M. F. Balli, S. Uludag, A. A. Selcuk, and B. Tavli, "Distributed multi-unit privacy assured bidding (PAB) for smart grid demand response programs," *IEEE Trans. on Smart Grid*, vol. 9, no. 5, 2018.
- [27] E. Dall'Anese, A. Bernstein, and A. Simonetto, "Feedback-based projected-gradient method for real-time optimization of aggregations of energy resources," in *2017 IEEE Global Conference on Signal and Information Processing (GlobalSIP)*, Montreal, Canada, Nov. 2017.
- [28] J. X. Chin, A. Bernstein, and G. Hug, "Online appendix for aggregating privacy-conscious DERs for grid service provision," 2019. [Online]. Available: <https://zenodo.org/record/3384772>
- [29] W. Kleiminger, C. Beckel, and S. Santini, "Household occupancy monitoring using electricity meters," in *Proceedings of the 2015 ACM International Joint Conference on Pervasive and Ubiquitous Computing (UbiComp 2015)*, Osaka, Japan, Sept. 2015.
- [30] J. Lofberg, "YALMIP : a toolbox for modeling and optimization in MATLAB," in *2004 IEEE International Conference on Computer Aided Control Systems Design*, New Orleans, LA, USA, Sept. 2004.
- [31] O. Tan, J. Gomez-Vilardebo, and D. Gündüz, "Privacy-cost trade-offs in demand-side management with storage," *IEEE Trans. on Information Forensics and Security*, vol. 12, no. 6, pp. 1458–1469, 2017.
- [32] J. X. Chin, G. Giacconi, T. Tinoco De Rubira, G. Hug, and D. Gündüz, "Considering time correlation in the estimation of privacy loss for consumers with smart meters," in *2018 Power System Computation Conference (PSCC)*, Dublin, Ireland, June 2018.
- [33] G. Eibl and D. Engel, "Influence of data granularity on smart meter privacy," *IEEE Trans. on Smart Grid*, vol. 6, no. 2, pp. 930–939, 2015.